

## Direct Resolution and Identification of the Sublattices in Compound Semiconductors by High-Resolution Transmission Electron Microscopy

A. Ourmazd, J. R. Rentschler, and D. W. Taylor  
*AT&T Bell Laboratories, Holmdel, New Jersey 07733*  
(Received 7 July 1986)

We describe a technique capable of directly resolving and identifying the sublattices occupied by the different constituents of compound semiconductors, under conditions which allow simple interpretation of the images. We present experimental lattice images of InP, GaP, and GaAs, which are direct representations of the sample structure and allow the simultaneous resolution and identification of the sublattices for the first time. We thus establish that the technique is applicable to all zinc-blende semiconductor compounds

PACS numbers: 61.16.Di, 61.55.Hg

Recent years have seen an increasing application of high-resolution transmission electron microscopy (HRTEM) to a wide range of materials problems. The advent of the new generation of HRTEM's has made possible the examination of semiconducting materials in a number of projections in addition to the usual  $\langle 110 \rangle$ , thereby overcoming one of the severe limitations imposed by the insufficient resolution of the previous generation. In particular, it is now possible to resolve individual atom columns in at least two important orientations, namely,  $\langle 100 \rangle$  and  $\langle 111 \rangle$ .<sup>1</sup> While this possibility is likely to be of decisive importance in achieving full structural analysis of elemental semiconductors, it is insufficient to yield a complete characterization of compound semiconductors. In addition to the resolution of the individual atomic columns, such a characterization requires the ability to *identify* the two fcc sublattices, which in the zinc-blende structure are occupied by different atom types. Since there is extensive evidence that defects occupying different sublattices exhibit widely different electronic and mechanical properties, the task of resolving *and* identifying the two sublattices is of primary scientific interest. In this paper we describe a method capable of achieving this goal and demonstrate the power of the technique by presenting the first HRTEM lattice images of InP, GaP, and GaAs, where the two sublattices are directly resolved and identified near optimum (Scherzer) defocus, where image interpretation is particularly simple.<sup>2</sup> Since the above compounds span essentially the entire range of atomic-number difference encountered in compound semiconductors, we thus establish the applicability of the technique to all zinc-blende compounds.

Because HRTEM lattice images reveal a two-dimensional projection of the structure, a distinction by lattice imaging between the columns occupied with different atom types is only possible when the different atomic columns parallel to the electron beam are not equally populated with all atom types. In the zinc-blende system, this requires the examination of the struc-

ture in either the  $\langle 110 \rangle$  or the  $\langle 100 \rangle$  projection, when the neighboring atomic columns are entirely occupied with different atomic species. Since the resolution of individual atom columns in the  $\langle 110 \rangle$  projection requires the transmission of information well beyond the point-to-point resolution of even the latest generation of HRTEM's, thus severely complicating reliable image interpretation, we restrict the discussion to the  $\langle 100 \rangle$  projection, which in any case is the most commonly utilized orientation of fabricated semiconductor systems. We have employed a JEOL model 4000-EX HRTEM operating at 400 kV, equipped with a computer-controlled on-line image simulation and processing station. Our preliminary evaluation of the TEM has yielded a point-to-point resolution of  $\sim 1.6 \text{ \AA}$ . The objective aperture used allowed the central, the four 200, and the four 220 beams to contribute to the image. Thus no information outside the point-to-point resolution of the microscope was used in formation of the lattice images.

The *resolution* of the two sublattices in the  $\langle 110 \rangle$  projection relies on the ability of modern HRTEM's faithfully to transmit, near Scherzer defocus,  $(1.5\lambda C_s)^{1/2}$ , the information contained in the 220 reflections of semiconductors. The 220 reflections, however, are not sensitive to small changes in the atomic number and therefore do not contain significant chemical information. The 200 reflections, on the other hand, are kinematically allowed in compound semiconductors only because the two sublattices are occupied by different atomic species, and are consequently extremely sensitive to chemical difference between the atomic constituents. In order to both resolve *and* to identify the two sublattices, the 200 and 220 beams must make comparable contributions to the lattice image, under conditions when their phase relationship is kinematical. Figure 1 describes the way the phases and amplitudes of these beams change with sample thickness in InP. The major difficulty in achieving simultaneous resolution and identification is due to the small amplitude of the 200 beams relative to the 220, in the thickness range where their phase relationship is ap-

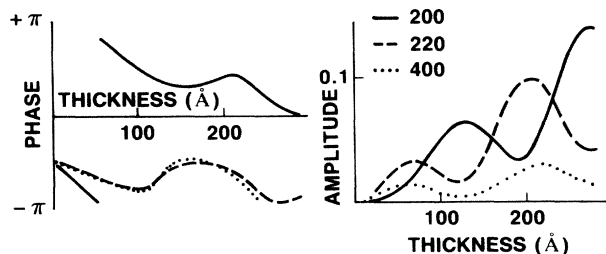


FIG. 1. *Pendellösung* plots of phases and amplitudes of beams for  $\langle 100 \rangle$  InP at 400 kV. The phases are with respect to the central beam.

proximately kinematical and hence the image is a simple representation of the sample structure. Therefore, in general, forming a  $\langle 100 \rangle$  lattice image of a compound semiconductor at Scherzer defocus in the "kinematical" (small thickness) region results only in strong 220 fringes, when no distinction between the atom types is possible *a priori* [see Fig. 4(b)]. On the other hand, a lattice image obtained in the region where the 200 reflection has acquired substantial intensity is not a simple representation of the sample structure, because of the nonkinematic phase relationship of the interfering beams. This dilemma can be overcome by our recognizing that the transmission of a beam by the lens and hence its contribution to the image is governed by its phase relative to the central beam, which can be controlled through the objective lens defocus.<sup>2</sup> This can be quantitatively described by means of the contrast transfer function (CTF) of the microscope. Figure 2 shows the CTF of our HRTEM at three defocus values around Scherzer ( $-460 \text{ \AA}$ ) for beams which bear a near-kinematic phase relationship to the central beam. The CTF essentially describes the way information is transmitted by the objective lens as a function of spatial frequency. Information with a frequency in those regions where the CTF is small is severely attenuated, while a CTF value of 1 implies unattenuated transmission of information. Since the 220 beams in semiconductors lie close to the first zero of the CTF, the contribution of these beams to the image can be conveniently controlled by small deviations of the defocus from the Scherzer value, provided that their phase with respect to the central beam is close to kinematic. Our proposed method relies on our obtaining lattice images in thickness regions where the kinematic phase relationship holds and reducing the 220 beam amplitude to levels comparable with that of the 200 by operating at defocus values less than, but close to, Scherzer. In this way, chemically sensitive images are obtained, which are simple to interpret and, as shown below, are direct representations of the sample structure. The exact defocus to be used will be determined by the relative amplitudes of the 200 and 220 beams and thus the difference in the atomic numbers of the constituents, the lattice parameter of the material, and, to some extent, its average atomic number

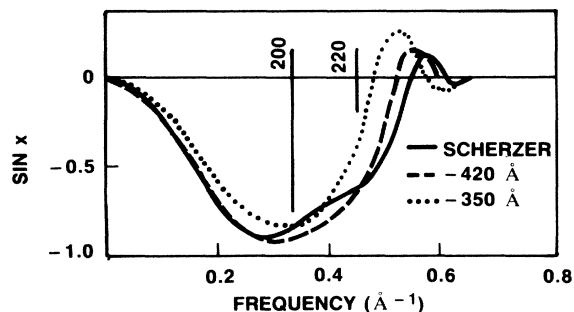


FIG. 2. Contrast transfer function of JEOL model 4000-EX TEM (including the damping envelope) for three defocus values near Scherzer ( $-460 \text{ \AA}$ ). The positions of two GaAs reflections are also indicated.

and the sample thickness.

Because of the large difference between the atomic numbers of its constituents (34), InP represents a particularly suitable system for the simultaneous resolution and identification of its two sublattices. Our image simulations<sup>3</sup> show that resolution and identification of the sublattices in InP are possible for thicknesses up to  $\sim 50 \text{ \AA}$  in the defocus range  $-420$  to  $-490 \text{ \AA}$ . Since samples with thicknesses below  $30 \text{ \AA}$  are in practice difficult to obtain, the more restrictive range of defocus values of  $-420$  to  $-460 \text{ \AA}$  must be employed. Figure 3 is an experimental lattice image of InP in the  $\langle 100 \rangle$  projection, where the two sublattices are directly resolved and identified. Optical diffractometry confirms the image to have been obtained near Scherzer defocus (see Fig. 4), thus indicating that the atom columns are black. We find a good fit to this image at a defocus of  $-430 \text{ \AA}$  and a thickness of  $38 \text{ \AA}$ , where the kinematic phase relationship between the beams holds. The image is thus a direct representation of the projected potential, with the heavier In atom columns appearing larger and darker than the lighter P columns. Confidence in the correct interpretation of HRTEM images can only be gained after a number of images have been successfully simulated.

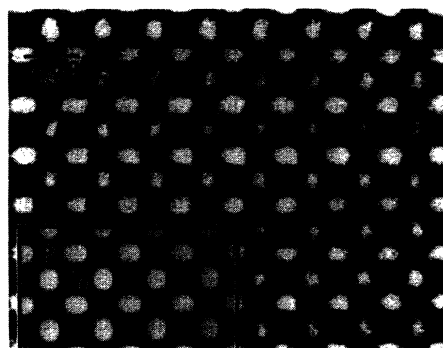


FIG. 3.  $\langle 100 \rangle$  lattice image of InP. Inset shows simulated image. Atom columns appear black, tunnels white. Note that heavier In atoms appear larger and darker than the lighter P.

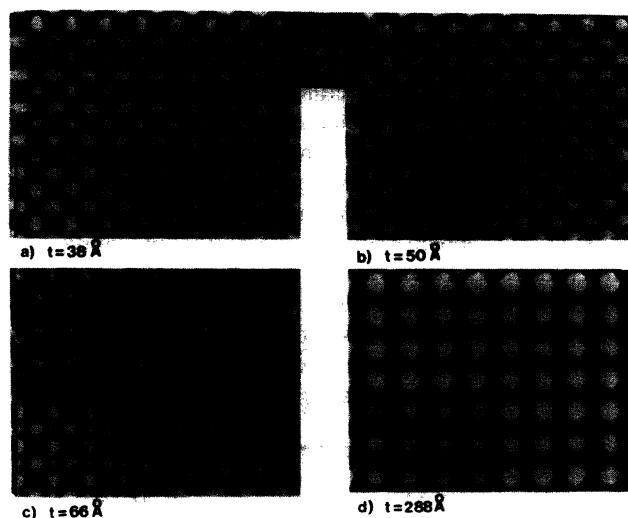


FIG. 4.  $\langle 100 \rangle$  images of InP at different sample thicknesses. Insets are simulated images and optical diffractogram, which confirms defocus to be near Scherzer.

Figure 4 shows a series of images (including that of Fig. 3) all recorded in a single exposure of a negative, i.e., obtained at the same defocus, from a wedge-shaped sample. These micrographs summarize the principal changes observed in the lattice image with increasing sample thickness. We have successfully obtained simulated fits by only allowing the thickness to change and checked our thickness assignments by using the *Pendellösung* oscillations of the central beam for calibration. It is through such detailed comparisons of experimental and simulated images that we ensure that the correct defocus is experimentally achieved. Our simulations allow us to be confident that the image of Fig. 3 is a direct representation of the sample projected potential. We have ascertained that when an image similar to that of Fig. 3 is obtained, the darker, larger blobs always correspond to the heavier In atom columns. Thus the identification of the two sublattices is free from ambiguity.

We have applied the same approach to the lattice imaging of GaP, whose constituents exhibit an atomic number difference of 16, which is intermediate in the range observed in compound semiconductors. Our simulations show the defocus "window" to extend from  $\sim -400$  to  $-440$  Å, with the two sublattices identifiable for sample thicknesses up to  $\sim 70$  Å. Figure 5 is an experimental lattice image of GaP where the sublattices are directly resolved and identified. We have again obtained satisfactory fits over a wide range of thicknesses, to ensure the reliability of our interpretation. We find experimentally and theoretically that at a slightly larger defocus ( $-490$  Å) and in the thickness range 60–70 Å, images similar to that of Fig. 4 can be obtained, with the important difference that the larger and darker blobs correspond to the lighter atoms and vice versa. On the basis of such an image alone, a totally incorrect identification



FIG. 5.  $\langle 100 \rangle$  lattice image of GaP. Insets are simulated image and optical diffractogram. Atom columns are black, with the heavier Ga appearing larger and darker than the lighter P. Thickness 40 Å, defocus  $-420$  Å.

of the atom types occupying each sublattice can be made. This difficulty can only be reliably overcome by fitting the experimental images over a range of thicknesses. In particular, correct identification of atom types can be ensured by ascertaining that images similar to that of Fig. 5 extend to the thinnest regions of the foil and are not preceded by images consisting of strong 220 fringes [similar to those of Fig. 4(b)]. This difference in the change of the images with thickness provides both a straightforward means of achieving a correct assignment and a demonstration of the importance of fitting HRTEM images over a range of parameters.

Since the difference between the atomic numbers of Ga and As is the smallest encountered in the compound semiconductors, GaAs represents the most challenging application of our technique. Because of this small difference, the 200 beams do not acquire appreciable amplitude until thickness in excess of 100 Å, when the kinematic phase relationship is far from being satisfied. The phases, however, resume a kinematic arrangement after the first *Pendellösung* oscillation of the 220 and 400 beams, i.e., in the thickness range 280–300 Å, when the 200 beams also contain appreciable intensity. Nevertheless, the 220 beams are still considerably stronger than the 200 and, in order to prevent them from dominating the image, their contribution must be attenuated by means of the CTF. This requires a defocus value in the range  $-350$  to  $-380$  Å. Figure 6 is the experimental lattice image of GaAs which again allows the identification of the two sublattices for the first time. By fitting images over a wide range of thickness, we have established that, once an image of this type is obtained, the larger, darker blobs are always associated with the heavier As atom columns, making the identification of the sublattices unambiguous. However, we find both experimentally and theoretically that the contrast of such images is poor, making their recognition in the course of an experimental difficult. In practice we have found this

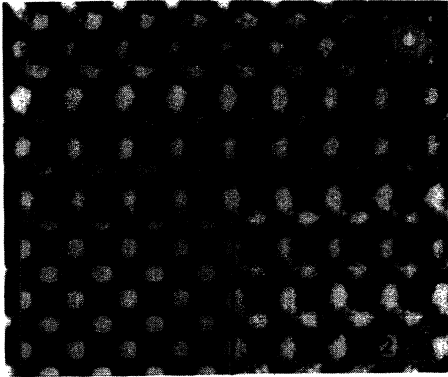


FIG. 6.  $\langle 100 \rangle$  lattice image of GaAs. Insets are simulated image and optical diffractogram. Atom columns are black, with the heavier As appearing larger and darker than the lighter Ga. Thickness 282 Å, defocus  $-360$  Å.

possible only through the extensive use of our on-line image processing and simulation system.

In conclusion, we have described a technique capable of directly resolving and identifying the individual atomic columns of a compound semiconductor, over the entire range of atomic-number difference encountered in this important class of materials. By presenting the first HRTEM lattice images of InP, GaP, and GaAs, where

the individual sublattices are directly resolved and identified, we have established the practicability of the technique and elucidated guidelines for its use on a routine basis. Our results show that, by careful but practicable control of microscope and sample parameters, it is now possible to achieve a complete structural characterization of all zinc-blende semiconductor compounds. Although the study of defects will require fresh modeling and simulation, our present work paves the way for the investigation of a wide range of important systems in semiconductors, such as heterostructures, interfaces, surfaces, and other defects, whose properties are likely to depend crucially on the sublattice they occupy.

<sup>1</sup>A. Ourmazd, K. Ahlborn, K. Ibeh, and T. Honda, *Appl. Phys. Lett.* **47**, 685 (1985).

<sup>2</sup>For a detailed discussion of HRTEM, see J. C. H. Spence, *Experimental High-Resolution Electron Microscopy* (Oxford Univ. Press, New York, 1980).

<sup>3</sup>Standard SHRLI (simulation of high-resolution lattice images) multislice algorithm. For a discussion, see Ref. 2, p. 143. 128 square array,  $C_s = 1$  mm,  $\Delta = 80$  Å, beam divergence  $= 0.7$  mrad. None of the simulated images depends sensitively on these parameters. For further simulated images of compound semiconductors, see P. G. Self, R. W. Glaisher, and A. E. C. Spargo, *Ultramicroscopy* **18**, 49 (1985).

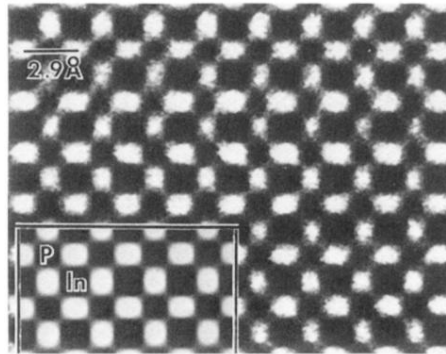


FIG. 3.  $\langle 100 \rangle$  lattice image of InP. Inset shows simulated image. Atom columns appear black, tunnels white. Note that heavier In atoms appear larger and darker than the lighter P.

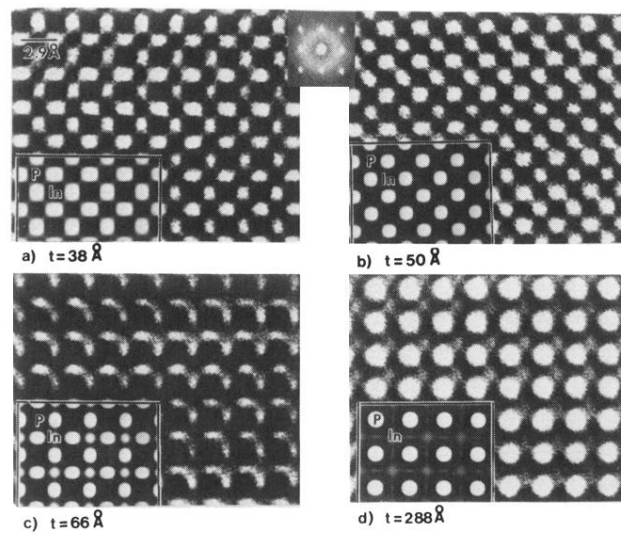


FIG. 4.  $\langle 100 \rangle$  images of InP at different sample thicknesses. Insets are simulated images and optical diffractogram, which confirms defocus to be near Scherzer.

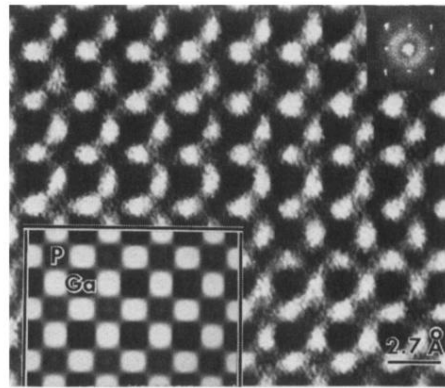


FIG. 5.  $\langle 100 \rangle$  lattice image of GaP. Insets are simulated image and optical diffractogram. Atom columns are black, with the heavier Ga appearing larger and darker than the lighter P. Thickness 40 Å, defocus  $-420$  Å.

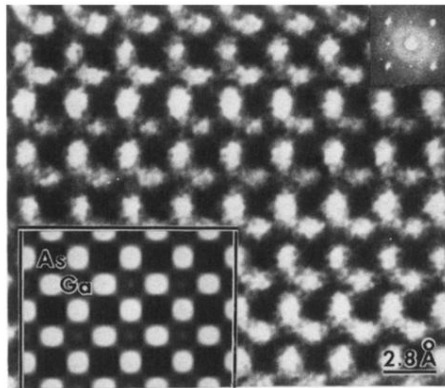


FIG. 6.  $\langle 100 \rangle$  lattice image of GaAs. Insets are simulated image and optical diffractogram. Atom columns are black, with the heavier As appearing larger and darker than the lighter Ga. Thickness 282 Å, defocus  $-360$  Å.